Defect-free Ge-on-insulator with (100), (110), and (111) orientations by growth-direction-selected rapid-melting growth

Toko, Kaoru
Department of Electronics, Kyushu University

Tanaka, Takanori
Department of Electronics, Kyushu University

Ohta, Yasuharu
Department of Electronics, Kyushu University

Sadoh, Taizoh
Department of Electronics, Kyushu University

他

出版情報：Applied Physics Letters. 97 (15), pp.152101(1)-152101(3), 2010-10. American Institute of Physics
バージョン：

Defect-free Ge-on-insulator with (100), (110), and (111) orientations by growth-direction-selected rapid-melting growth

Kaoru Toko, Takanori Tanaka, Yasuharu Ohta, Taizoh Sadoh,[a] and Masanobu Miyao[b]
Department of Electronics, Kyushu University, 744 Motooka, Fukuoka 819-0395, Japan

(Received 23 July 2010; accepted 1 September 2010; published online 11 October 2010)

Defect-free Ge-on-insulator (GOI) with various crystal orientations is essential to realize high-speed and multifunctional devices. Seeded rapid-melting growth of GOI is investigated as a function of seed-orientations and growth-directions. From (100)-oriented Si seeds, Ge growth with a (100) orientation propagates for all growth-directions, however, rotational-growth is observed for some directions when Si seeds with (110) and (111) orientations are used. Such rotational-growth can be completely suppressed by selecting the growth-directions deviating from ⟨111⟩ by more than 35°. Transmission-electron-microscopy observation shows no-stacking fault and no-dislocations. Consequently, defect-free GOI with (100), (110), and (111) orientation is achieved, which demonstrates high-hole mobility (~1100 $cm^2/V\,s$). © *2010 American Institute of Physics*. [doi:10.1063/1.3493184]

Single crystalline Ge is an attractive channel material for high-speed metal-oxide-semiconductor (MOS) transistors as it provides much higher carrier mobility compared to Si.[1,2] Thin-body Ge-on-insulator (GOI) channels can provide further high-performance operation under the advantages of low parasitic capacitance and low leakage current.[3] Consequently, high-quality GOI structures should be developed in the next-generation ultralarge scale integrated circuit (ULSI) technology. The oxidation-induced Ge condensation method is considered to be a promising technique.[4,5] However, defect-originated holes with the concentration of 10^{17} cm^{-3} were generated during the oxidation, which resulted in low carrier mobility (410 $cm^2/V\,s$).[6]

Recently, the seeding rapid-melting-growth of amorphous-Ge (*a*-Ge) was examined to obtain GOI structures, where *a*-Ge layers deposited on SiO_2 films were first grown vertically from Si substrates through opening windows formed in SiO_2 films, and then propagated laterally over SiO_2. These efforts achieved defect-free (100) Ge stripes (20–40 μm length, 2–3 μm width) on SiO_2.[6–9] We investigated this process, and clarified that the driving force to cause lateral growth is the spatial gradient of the solidification temperature originating from Si–Ge mixing at seeding areas.[10] Furthermore, we optimized the sample structures and annealing conditions, which achieved the (100) GOI with high hole mobility (1040 $cm^2/V\,s$).[11,12] In addition, giant (~400 μm) growth exceeding one order longer than literatures[6–9] was obtained, which enabled the ULSI application of this method.

To extend the application fields of this method, GOI growth with various crystal orientations should be established. Since the electron and hole mobility of Ge show the highest values in (111) and (110) orientations, respectively,[13] future ultrahigh-speed MOS transistors require the GOI with (111) and (110) orientations. In addition, recently, high quality epitaxial growth of ferromagnetic (Fe_3Si, Fe_2MnSi, Co_2FeSi)[14–16] and optical (GaN)[17] materials were reported on (111) Ge. Consequently, GOI crystals with such various orientations should be the powerful platform to merge spin-transistors and opto-devices with ultrahigh speed MOS transistors.

In this paper, rapid-melting growth for GOI with (111) and (110) orientations are examined. The growth characteristics are investigated as a function of Si-seed orientation [(111), (110), and (100)] and growth-directions. Unexpected rotational-growth of Ge stripes is found depending on seed-orientations and growth-directions. Based on the bonding strength between various lattice planes, the growth conditions to prevent such rotational-growth are found. This achieves defect-free single-crystal GOI stripes with all crystal orientations [(100), (110), and (111)].

In the experiments, Si (100), (110), and (111) substrates (600 μm thickness) covered with SiO_2 films (30–50 nm thickness) or Si_3N_4 films (100 nm thickness) were used. These films were patterned by wet etching to form seeding areas (150×30 μm^2), where square seeds with various patterning direction were formed. Subsequently, *a*-Ge layers (100 nm thickness) were deposited using a molecular beam epitaxy system (base pressure: 5×10^{-11} Torr), and they were patterned into narrow stripe lines (400 μm length, 3 μm width). The sample structure is schematically shown in Fig. 1(a), where the angle θ of the growth direction of a stripe was defined as the angle from the direction of the orientation flatness, i.e., the ⟨011⟩ direction for all substrate orientations. Then SiO_2 layers (800 nm thickness) were deposited by sputtering. Finally, these samples were heat-treated by rapid thermal annealing (RTA) at 1000 °C (1 s) to induce melting growth from the seeding areas. Morphology, crystal orientation, and crystal quality of grown layers were characterized by Nomarski optical microscopy, cross-sectional transmission electron microscopy (X-TEM), and electron backscattering diffraction (EBSD), where the capping SiO_2 layers were removed by wet-etching before the EBSD measurements. Carrier mobility was evaluated by measuring the temperature dependence of the electrical conductivity, as described in the previous work.[10,11]

A typical Nomarski optical micrograph of the annealed sample (substrate: SiO_2/(100)Si, θ=0°) is shown in Fig. 1(b),

[a]Electronic mail: sadoh@ed.kyushu-u.ac.jp.
[b]Electronic mail: miyao@ed.kyushu-u.ac.jp.

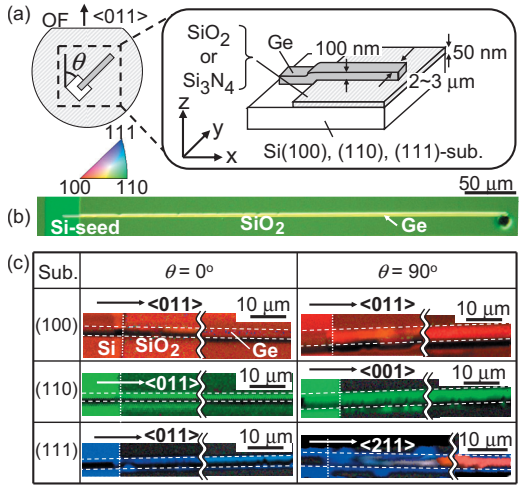

FIG. 1. (Color) (a) Schematic sample structure, (b) Nomarski optical micrograph of the sample [substrate: Si (100), θ:0°] after RTA (1000 °C, 1 s), and (c) EBSD images of grown regions near seeding edges and at around 100 μm from seeding edge [substrate: Si (100), (110), and (111), θ:0°,90°].

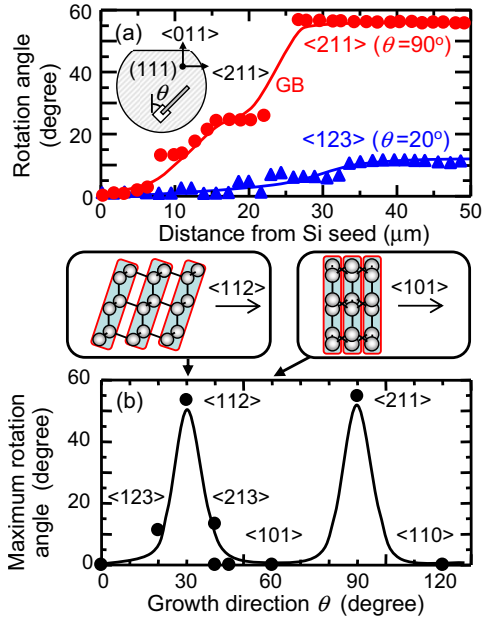

FIG. 2. (Color online) (a) Rotation angle as a function of the distance from seeding edge for different growth-directions [substrate: Si (111), direction: ⟨211⟩ and ⟨123⟩], and (b) maximum rotation angle as a function of the growth direction [substrate: Si (111)]. Crystal planes and their bonding structures along ⟨112⟩ and ⟨101⟩ directions are also shown.

which indicates the formation of a uniform and flat Ge stripe with 400 μm length. Such uniform structures were obtained for all samples (substrate: SiO_2/(100), (110), (111) Si, Si_3N_4/(100), (110), (111) Si, θ=0°–90°). Growth-direction dependent EBSD images (θ=0°,90°) of the Ge stripes formed on the SiO_2 layers with Si (100), (110), and (111) seeding substrates are summarized in Fig. 1(c), where images near the seeding edges and at 100 μm away from the seeds are displayed. Color mapping in the images represents the crystal orientation perpendicular to the sample surface, i.e., z-axis in Fig. 1(a). Crystal orientations near the seeding edges are found to be identical to Si substrates for all samples. This clearly means that crystal growth is initiated at Si seeding areas and propagates laterally over SiO_2 films. For θ=0°, these crystal orientations of all samples are kept constant even at 100 μm away from the seeds, as shown in Fig. 1(c). Such stabilized lateral growth is also obtained for Ge stripes with θ=90°, as far as the growth is initiated from the Si (100) and (110) substrates. However, the growth initiated from the Si (111) substrate gradually changes its orientation along the lateral growth path and reaches to the (100) orientation. Detailed analysis of the EBSD measurements indicated that the crystal orientation parallel to the growth direction (x-axis) was kept ⟨211⟩ throughout the growth. These results suggest that the lateral growth propagates with rotating its orientation, when special growth conditions are chosen for the experiments, i.e., Si (111) substrate and θ=90°.

To investigate the rotational-growth phenomena in more detail, the rotation angles of the crystal orientation in z-axis were evaluated as a function of the distance from the seeding edges [substrate: SiO_2/Si (111)]. Figure 2(a) shows the results for the growth aligned to ⟨211⟩ (θ=90°) and ⟨123⟩ (θ=20°) directions. In the former case, the rotation angle increases from 0° to 60° with increasing distance from 0 to 30 μm. At 20 μm, we can see a plateau, which coincides with the generation of grain boundary, as shown in Fig. 1(c). In the latter case, however, the increase in rotation angle is very gentle, i.e., 0° to 12° in the region between 0 to 50 μm. Figure 2(b) shows the maximum rotation angles of the crystal orientation as a function of the growth direction (θ). It is clear that the rotation angles show maximum values for the ⟨112⟩ and its equivalent directions, and changes with a 60° period reflecting the crystal symmetry of the Ge(111) plane.

Now, let us discuss the driving force to cause the lateral rotational-growth. In 1980s, microzone melting growth of Ge has been intensively examined which demonstrated the preferential (100) Ge growth on SiO_2 films. This was attributed to the lowest interfacial free energy between (100) Ge and SiO_2 layers.[18] In addition, crystal cleavage experiments indicated that the weakest bonding strength in the diamond crystal structure exists between (111) planes.[19] From these results, we can speculate that the Ge crystal initiated from (111) and (110) orientation should propagate rotationally to minimize the Ge/SiO_2 interface free energy by slipping between the (111) planes. Since the (112) plane is much closed to the (111) plane, significant rotation is observed for Ge stripes aligned to the ⟨112⟩ direction. These situations are displayed in the insets of Fig. 2(b).

In order to examine the validity of this speculation, we explore the rotational growth for Ge stripes using Si (110) seeding substrates. Figures 3(a) and 3(b) show the EBSD images of Ge stripes aligned to the ⟨111⟩ and ⟨121⟩ directions (θ=35° and 30°), respectively, where images obtained near the seeding edges and at 100 μm away from the seeds are compared. Rotational growth in the vicinity of ⟨111⟩ direction predicted in our speculation is clearly observed in these two figures. Similar experiments using Ge stripes grown on Si (100) was also carried out. No rotational growth was observed for samples with various growth directions (θ=0°, 30°, 45°, 60°, and 90°), which supported the stabilized Ge (100) thin films on SiO_2 layers.

The maximum rotation angles of the crystal orientation of Ge surfaces are summarized as a function of the angle between the growth direction and the ⟨111⟩ direction. They are shown in Fig. 3(c), where data obtained from Ge stripes grown on the Si (111), (110), and (100) seeding substrates are compared. It is particularly worth noting that rotating

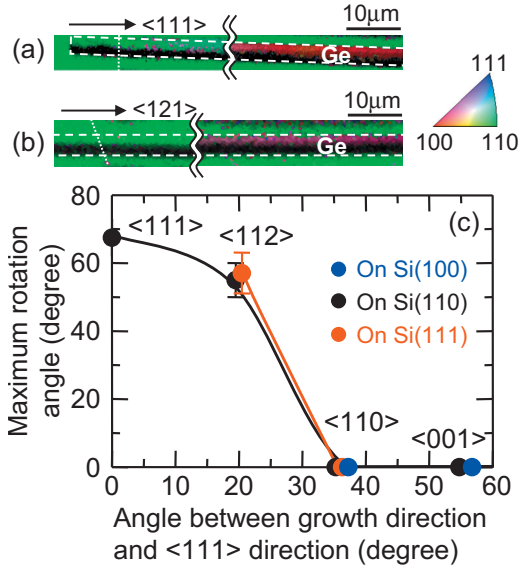

FIG. 3. (Color) EBSD images for samples [θ=30° (a), 35° (b)] grown on Si (110) seeding substrates and (c) maximum rotation angle as a function of the angle deviating from ⟨111⟩ direction. Results obtained from Si (100), (110), and (111) seeding substrates are summarized.

growth can be completely suppressed by selecting the growth directions deviating from the ⟨111⟩ direction by more than 35°. This is an important guiding principle to obtain rotation-free GOI with (100), (110), and (111) orientations.

Finally, we demonstrate the formation of high quality GOI with (100), (110), and (111) orientation. Ge stripes are grown on SiO_2 or Si_3N_4 by using Si (100), (110), and (111) substrates as growth seeds, where all growth directions are selected as ⟨011⟩. Figure 4 shows the TEM images of grown regions 100 μm away from the seeding areas together with the electron diffraction (ED) patterns. No dislocation or stacking fault is detected in all TEM images. In addition, ED patterns show the Ge orientation identical to that in Si seeding substrates. This clearly indicates that melting-growth seeded at Si substrates propagates over SiO_2 or Si_3N_4 without any rotation. This is a big advantage of growth-direction-selected rapid-melting growth.

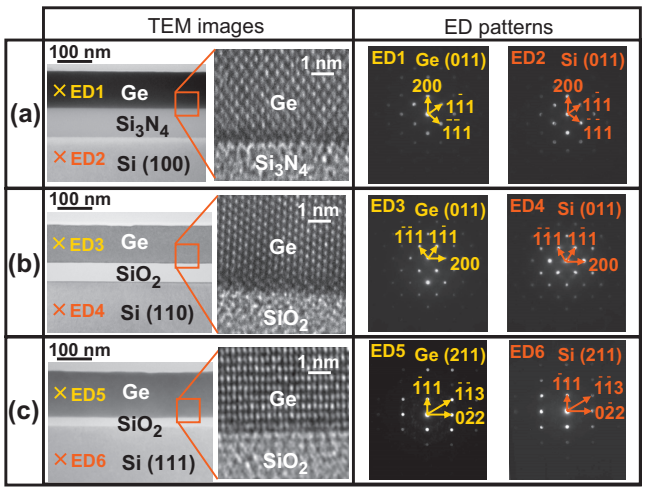

FIG. 4. (Color) TEM images and ED patterns of GOI samples grown from Si (100) (a), (110) (b), and (111) seeding substrates (c). All growth directions are fixed as ⟨011⟩.

The electrical characteristics were also evaluated. Thermoelectromotive-force-method measurements clearly indicated that all Ge stripes were p-type conduction. Hole-generation ($\sim 5\times10^{16}$ cm^{-3}) originated from point defects was significantly lower than that obtained by the oxidation-induced Ge condensation process ($\sim 1.3\times10^{17}$ cm^{-3}).[5] As a result, high hole mobility ($\sim$1100 $cm^2/V\,s$) exceeding conventional methods ($\sim$410 $cm^2/V\,s$) was realized. In this way, high mobility defect-free Ge stripes with (100), (110), and (111) orientations are achieved on SiO_2 or Si_3N_4 films.

In summary, rapid-melting growth features of GOI initiated from (100), (110), and (111) Si substrates have been comprehensively studied as a function of lateral-growth directions. It is clarified that the growth propagates continuously keeping their seed-orientation by selecting the growth direction deviating from ⟨111⟩ by more than 35°. This achieves defect free GOI with various crystal orientations, i.e., (100), (110), and (111) orientations. Such a variety of high quality GOI will be a useful platform for high-speed and multifunctional devices.

A part of this work was supported by Semiconductor Technology Academic Research Center (STARC) and a Grant-in-Aid for Scientific Research from the Ministry of Education, Culture, Sport, Science, and Technology in Japan. Valuable comments by Dr. I. Mizushima, Dr. N. Tamura, and Dr. M. Yoshimaru of STARC are greatly appreciated.

[1]M. Miyao, E. Murakami, H. Etoh, K. Nakagawa, and A. Nishida, J. Cryst. Growth **111**, 912 (1991).
[2]C. H. Lee, T. Nishimura, N. Saido, K. Nagashio, K. Kita, and A. Toriumi, Tech. Dig. - Int. Electron Devices Meet. **2009**, 457.
[3]T. Maeda, K. Ikeda, S. Nakaharai, T. Tezuka, N. Sugiyama, Y. Moriyama, and S. Takagi, IEEE Electron Device Lett. **26**, 102 (2005).
[4]N. Sugiyama, T. Tezuka, T. Mizuno, M. Suzuki, Y. Ishikawa, N. Shibata, and S. Takagi, J. Appl. Phys. **95**, 4007 (2004).
[5]T. Maeda, K. Ikeda, S. Nakaharai, T. Tezuka, N. Sugiyama, Y. Moriyama, and S. Takagi, Thin Solid Films **508**, 346 (2006).
[6]Y. Liu, M. D. Deal, and D. Plummer, Appl. Phys. Lett. **84**, 2563 (2004).
[7]D. J. Tweet, J. J. Lee, J. S. Maa, and S. T. Hsu, Appl. Phys. Lett. **87**, 141908 (2005).
[8]S. Balakumar, M. M. Roy, B. Ramamurthy, C. H. Tung, G. Fei, S. Tripathy, C. Dongzhi, R. Kumar, N. Balasubramanian, and D. L. Kwong, Electrochem. Solid-State Lett. **9**, G158 (2006).
[9]T. Hashimoto, C. Yoshimoto, T. Hosoi, T. Shimura, and H. Watanabe, Appl. Phys. Express **2**, 066502 (2009).
[10]M. Miyao, T. Tanaka, K. Toko, and M. Tanaka, Appl. Phys. Express **2**, 045503 (2009).
[11]M. Miyao, K. Toko, T. Tanaka, and T. Sadoh, Appl. Phys. Lett. **95**, 022115 (2009).
[12]K. Toko, M. Kurosawa, H. Yokoyama, N. Kawabata, T. Sakane, Y. Ohta, T. Tanaka, T. Sadoh, and M. Miyao, Appl. Phys. Express **3**, 075603 (2010).
[13]T. Low, M. F. Li, G. Samudra, Y. C. Yeo, C. Zhu, A. Chin, and D. L. Kwong, IEEE Trans. Electron Devices **52**, 2430 (2005).
[14]T. Sadoh, M. Kumano, R. Kizuka, K. Ueda, A. Kenjo, and M. Miyao, Appl. Phys. Lett. **89**, 182511 (2006).
[15]K. Hamaya, H. Itoh, O. Nakatsuka, K. Ueda, K. Yamamoto, M. Itakura, T. Taniyama, T. Ono, and M. Miyao, Phys. Rev. Lett. **102**, 137204 (2009).
[16]K. Kasahara, K. Yamamoto, S. Yamada, T. Murakami, K. Hamaya, K. Mibu, and M. Miyao, J. Appl. Phys. **107**, 09B105 (2010).
[17]R. R. Lieten, S. Degroote, M. Leys, and G. Borghs, J. Cryst. Growth **311**, 1306 (2009).
[18]K. Sakano, K. Moriwaki, H. Aritome, and S. Namba, Jpn. J. Appl. Phys., Part 2 **21**, L636 (1982).
[19]S. M. Sze, *Physics of Semiconductor Devices*, 2nd ed. (Wiley, New York, 1981), Chap. 1, p. 11.